On Variance-Reduced Simulations of the Boltzmann Transport Equation for Small-Scale Heat Transfer Applications

Nicolas G. Hadjiconstantinou

Gregg A. Radtke

Lowell L. Baker

Department of Mechanical Engineering,
Massachusetts Institute of Technology,
Cambridge, MA 02139

We present and discuss a variance-reduced stochastic particle simulation method for solving the relaxation-time model of the Boltzmann transport equation. The variance reduction, achieved by simulating only the deviation from equilibrium, results in a significant computational efficiency advantage compared with traditional stochastic particle methods in the limit of small deviation from equilibrium. More specifically, the proposed method can efficiently simulate arbitrarily small deviations from equilibrium at a computational cost that is independent of the deviation from equilibrium, which is in sharp contrast to traditional particle methods. The proposed method is developed and validated in the context of dilute gases; despite this, it is expected to directly extend to all fields (carriers) for which the relaxation-time approximation is applicable.
[DOI: 10.1115/1.4002028]

1 Introduction and Motivation

Particle-mediated energy transport in the transition regime between the ballistic and diffusive limits has recently received significant attention in connection to micro- and nanoscale science and technology [1]. Applications can be found in a variety of diverse fields such as thin semiconductor films [2,3] and superlattices [1], ultrafast processes [4,5], convective heat transfer [6,7], and gas-phase damping [8,10].

For a considerable number of applications, a classical description using the Boltzmann transport equation represents a good compromise between fidelity and complexity [1]. However, a numerical solution of the Boltzmann equation remains a formidable task due to the complexity associated with the collision operator and the high dimensionality of the distribution function. Both these features have contributed to the prevalence of particle solution methods, which are typically able to simulate the collision operator through simple and physically intuitive stochastic processes while employing importance sampling, which reduces computational cost and memory usage [11]. Another contributing factor to the wide usage of particle schemes is their natural treatment of the advection operator, which results in a numerical method that can easily handle and accurately capture traveling discontinuities in the distribution function [11]. An example of such a particle method is direct simulation Monte Carlo (DSMC) [12], which has become the standard simulation method for dilute gas flow. Methods that are similar in spirit have also been used for simulating phonon transport in solid state devices [13,14].

One of the most important disadvantages of particle methods for solving the Boltzmann equation derives from their reliance on statistical averaging for extracting field quantities from particle data [13,15]. In simulations of processes close to equilibrium, thermal noise typically exceeds the available signal. When coupled with the slow convergence of statistical sampling (statistical error decreases with the square root of the number of samples), this often leads to computationally intractable problems [15].

The present paper describes a particle simulation framework that alleviates the above disadvantages to a considerable extent while retaining the basic (and desirable) features of particle methods. This is achieved by simulating only the deviation from equilibrium, as originally proposed in Ref. [11]. Subsequent work [16] has shown that deviational methods (particle methods simulating the deviation from equilibrium) using the original Boltzmann (hard-sphere) collision operator require particle cancellation to prevent the number of simulated particles from growing in an unbounded manner. A stable deviational method (that does not require particle cancellation) for the hard-sphere gas was first developed in Refs. [17,18]; in that work, it was shown that the growth in the number of simulated particles observed in the collision-dominated regime when using the traditional hard-sphere collision operator [16] can be overcome using a special (but equivalent) form of the hard-sphere collision operator first derived by Hilbert [19]. In this paper, we exploit this observation to develop a deviational method for simulating the Boltzmann equation in the relaxation-time approximation. The method presented here considers the deviation from a suitably defined *global* equilibrium distribution and appears to be stable (does not require particle cancellation) for typical deviations from equilibrium.

2 Background

The Boltzmann transport equation is used to describe (under appropriate conditions) transport processes in a wide variety of fields [1], including dilute gas flow [20], phonon [21], electron [22], neutron [23], and photon transport [24]. It may be written as

$$\frac{\partial f}{\partial t} + \mathbf{c} \cdot \frac{\partial f}{\partial \mathbf{r}} + \mathbf{a} \cdot \frac{\partial f}{\partial \mathbf{c}} = \left[\frac{df}{dt} \right]_{\text{coll}} \tag{1}$$

where $f(\mathbf{r},\mathbf{c},t)$ is the single-particle distribution function [20], $[df/dt]_{\text{coll}}(\mathbf{r},\mathbf{c},t)$ denotes the collision operator, $\mathbf{r}=(x,y,z)$ is the position vector in physical space, $\mathbf{c}=(c_x,c_y,c_z)$ is the molecular velocity vector, $\mathbf{a}=(a_x,a_y,a_z)$ is the acceleration due to an exter-

Contributed by the Heat Transfer Division of ASME for publication in the JOURNAL OF HEAT TRANSFER. Manuscript received January 21, 2009; final manuscript received April 12, 2010; published online August 13, 2010. Assoc. Editor: Kenneth Goodson.

nal field, and t is time. In this paper, we focus on the relaxation-time approximation [20,1]

$$\left[\frac{df}{dt}\right]_{\text{coll}} = -\frac{1}{\tau}(f - f^{\text{loc}}) \tag{2}$$

where $f^{\text{loc}}(\mathbf{r},\mathbf{c},t)$ is the *local equilibrium* distribution function and τ is the relaxation time.

To focus the discussion, we specialize our treatment to the dilute gas case;[1] however, we hope that this exposition can serve as a prototype for the development of similar techniques in all fields where the relaxation-time approximation is applicable. In the interest of simplicity, in the present paper we assume $\tau \neq \tau(\mathbf{c})$ and that no external forces are present. The first assumption can be easily relaxed, as discussed in Sec. 3.1. External fields also require only relatively straightforward modifications to the algorithm presented below.

A dilute gas in equilibrium is described by a Maxwell–Boltzmann distribution, leading to a local equilibrium distribution

$$f^{\text{loc}} = \frac{n_{\text{loc}}}{\pi^{3/2} c_{\text{loc}}^3} \exp\left(-\frac{\|\mathbf{c} - \mathbf{u}_{\text{loc}}\|^2}{c_{\text{loc}}^2}\right) \tag{3}$$

which is parametrized by the local number density $n_{\text{loc}} = n_{\text{loc}}(\mathbf{r},t)$, the local flow velocity $\mathbf{u}_{\text{loc}} = \mathbf{u}_{\text{loc}}(\mathbf{r},t)$, and the most probable speed $c_{\text{loc}}(\mathbf{r},t) = \sqrt{2k_B T_{\text{loc}}/m}$ based on the local temperature $T_{\text{loc}} = T_{\text{loc}}(\mathbf{r},t)$. Here, k_B is Boltzmann's constant, and m is the molecular mass.

3 Variance Reduction Formulation

In a recent paper [11], Baker and Hadjiconstantinou showed that significant variance reduction can be achieved by simulating only the deviation $f^d(\mathbf{r},\mathbf{c},t) \equiv f - f^e$ from an *arbitrary*, but judiciously chosen, underlying equilibrium distribution $f^e(\mathbf{r},\mathbf{c},t)$. By adopting this approach, it is possible to construct Monte Carlo simulation methods [11,16,17,25] that can capture arbitrarily small deviations from equilibrium at a computational cost that is *small* and independent of the magnitude of this deviation. This is in sharp contrast to regular Monte Carlo methods, such as DSMC, whose computational cost for the same signal-to-noise ratio increases *sharply* [15] as the deviation from equilibrium decreases.

In the work that follows, the underlying equilibrium distribution (f^e) will be identified with absolute equilibrium,

$$f^e \equiv F(\mathbf{c}) = \frac{n_0}{\pi^{3/2} c_0^3} \exp\left[-\frac{\mathbf{c}^2}{c_0^2}\right] \tag{4}$$

where n_0 is a reference (equilibrium) number density and $c_0 = \sqrt{2k_B T_0/m}$ is the most probable molecular speed based on the reference temperature T_0. For small deviations from equilibrium, the choice of an appropriate reference equilibrium is straightforward but necessary. If deviations from the reference equilibrium are large, either due to strong nonlinearity in the problem or an inappropriate choice of reference equilibrium, the simulation method becomes less efficient than DSMC due to the large number of particles required to simulate the deviation from equilibrium.

Particle methods, such as DSMC, typically solve the Boltzmann equation by applying a splitting scheme,[2] in which molecular motion is simulated as a series of collisionless advection and collision steps of length Δt. In such a scheme, the collisionless advection step integrates

$$\frac{\partial f}{\partial t} + \mathbf{c} \cdot \frac{\partial f}{\partial \mathbf{r}} = 0 \tag{5}$$

by simply advecting particles for a time step Δt, while the collision step integrates

$$\frac{\partial f}{\partial t} = \left[\frac{df}{dt}\right]_{\text{coll}} \tag{6}$$

by changing the distribution by an amount of $[df/dt]_{\text{coll}}\Delta t$. Spatial discretization is introduced by treating collisions as spatially homogeneous within (small) computational cells of volume $\mathcal{V}_{\text{cell}}$.

Our approach retains this basic structure although it must be noted that since computational particles represent the deviation from equilibrium, they may be positive or negative, depending on the sign of the deviation from equilibrium at the location in phase space where they reside. As in other particle schemes [12], in the interest of computational efficiency, each *computational* deviational particle represents an *effective number* N_{eff} of physical deviational particles. Below we discuss the two main steps in more detail.

3.1 Collision Step. The variance-reduced form of Eq. (6) can be written as

$$\left[\frac{df}{dt}\right]_{\text{coll}} = \frac{1}{\tau}(f^{\text{loc}} - F) - \frac{1}{\tau} f^d \tag{7}$$

Within each computational cell, we integrate Eq. (7) using a two-part process. This integration requires local (cell) values of various quantities, denoted here by hats, which are updated every time step by sampling the instantaneous state of the gas.

In the first part, we remove a random sample of particles by deleting particles with probability $\Delta t/\hat{\tau}$ to satisfy

$$\tilde{f}^d(t + \Delta t) = \hat{f}^d(t) - \frac{\Delta t}{\hat{\tau}} \hat{f}^d(t) \tag{8}$$

In our implementation, this is achieved through an acceptance-rejection process, which can also treat the case $\hat{\tau} = \hat{\tau}(\mathbf{c})$.

In the second part, we create a set of positive and negative particles (using an acceptance-rejection process) to satisfy

$$\hat{f}^d(t + \Delta t) = \tilde{f}^d(t + \Delta t) + \frac{1}{\hat{\tau}}[\hat{f}^{\text{loc}}(t) - F]\Delta t \tag{9}$$

This step can be achieved by the following procedure. Let c_c be a (positive) value such that $\hat{f}^{\text{loc}}(\mathbf{c}) - F(\mathbf{c})$ is negligible for $\|\mathbf{c}\|_1 > c_c$, where $\|\cdot\|_1$ is an L^1-norm. Furthermore, let $\Delta_{\max}$ bound $|\hat{f}^{\text{loc}}(\mathbf{c}) - F(\mathbf{c})|$ from above. Then, repeat $\mathcal{N}_c$ times:

1. Generate uniformly distributed, random velocity vectors $\mathbf{c}$ with $\|\mathbf{c}\|_1 < c_c$.
2. If $|\hat{f}^{\text{loc}}(\mathbf{c}) - F(\mathbf{c})| > \mathcal{R}\Delta_{\max}$, create a particle with velocity $\mathbf{c}$ at a randomly chosen position within the cell and sign $\text{sgn}[\hat{f}^{\text{loc}}(\mathbf{c}) - F(\mathbf{c})]$. Here, $\mathcal{R}$ is a random number uniformly distributed on [0,1].

To find $\mathcal{N}_c$, we note that the number of particles (of all velocities and signs) that should be generated in a cell to obtain the proper change in the distribution function is

$$\frac{\Delta t}{N_{\text{eff}}} \int_{\mathcal{V}_{\text{cell}}} \int_{\mathbf{R}^3} \frac{|f^{\text{loc}} - F|}{\tau} d^3\mathbf{c} d^3\mathbf{r} = \frac{\Delta t \mathcal{V}_{\text{cell}}}{N_{\text{eff}} \hat{\tau}} \int_{\mathbf{R}^3} |\hat{f}^{\text{loc}} - F| d^3\mathbf{c} \tag{10}$$

where $\mathcal{V}_{\text{cell}}$ is the cell volume. The (expected) total number of particles ultimately generated by the above algorithm is

[1] Within the rarefied gas dynamics literature, the relaxation-time approximation is known as the BGK model [20].

[2] Note that a symmetrized algorithm typically provides higher-order accuracy. See Refs. [8,9] and references therein.

$$\mathcal{N}_c \frac{\int_{\mathbf{R}^3} |\hat{f}^{\mathrm{loc}} - F| d^3\mathbf{c}}{\Delta_{\max} 8 c_c^3} \tag{11}$$

By equating the above two expressions, we obtain $\mathcal{N}_c = 8\Delta t \Delta_{\max} \mathcal{V}_{\mathrm{cell}} c_c^3 / (\hat{\tau} N_{\mathrm{eff}})$.

3.2 Advection Step. It can be easily verified that when the underlying equilibrium distribution is not a function of space or time, as is the case here,

$$\frac{\partial f}{\partial t} + \mathbf{c} \cdot \frac{\partial f}{\partial \mathbf{r}} = \frac{\partial f^d}{\partial t} + \mathbf{c} \cdot \frac{\partial f^d}{\partial \mathbf{r}} \tag{12}$$

and thus the advection step for deviational particles is identical to that of physical particles.

Boundary condition implementation, however, is slightly more complex because the mass flux to system boundaries includes contributions from deviational particles as well as the underlying equilibrium distribution. Our implementation is discussed in more detail below.

3.2.1 Boundary Condition Implementation. Here, we extend previous work on diffuse boundary conditions to the more general case of the Maxwell accommodation model with accommodation coefficient α. According to this model, a fraction α of the molecules impacting the boundary are accommodated (diffusely reflected), while the remaining particles are specularly reflected.

Let $\boldsymbol{u}_b$ and c_b represent the boundary velocity and the most probable speed based on the boundary temperature, respectively. Let us assume, without loss of generality, that the boundary is parallel to the y-z plane and that the gas lies to the right ($x>0$) of the wall. For simplicity, let us also assume that the boundary does not move in the direction normal to its plane; i.e., the x-component of $\boldsymbol{u}_b$ is zero. Under these conditions, the Maxwell boundary condition can be written [26] as

$$f(c_x, c_y, c_z) = (1-\alpha) f(-c_x, c_y, c_z) + \alpha n_b \phi^b(c_x, c_y, c_z), \quad c_x > 0 \tag{13}$$

where in order to simplify the notation we have suppressed the space and time dependence of the distribution function. Here, $\phi^b(c_x, c_y, c_z) = (\pi c_b^2)^{-3/2} \exp(-\|\mathbf{c} - \boldsymbol{u}_b\|^2 / c_b^2)$; the quantity n_b is determined by mass conservation at the wall, namely,

$$\int_{c_x<0} c_x f d^3\mathbf{c} = -n_b \int_{c_x>0} c_x \phi^b d^3\mathbf{c} \tag{14}$$

Equation (13) can be written as

$$f^d(c_x, c_y, c_z) = (1-\alpha) f^d(-c_x, c_y, c_z) + \alpha[n_b \phi^b - F](c_x, c_y, c_z), \quad c_x > 0 \tag{15}$$

The algorithm used here for evaluating n_b considers deviational particles and the flux of particles due to the underlying equilibrium distribution $f^e \equiv F$ separately. More specifically, by introducing $n_b = n_b^e + n_b^d$ in Eq. (15), we obtain

$$f^d(c_x, c_y, c_z) = (1-\alpha) f^d(-c_x, c_y, c_z) + \alpha n_b^d \phi^b(c_x, c_y, c_z) + \alpha[n_b^e \phi^b(c_x, c_y, c_z) - F(c_x, c_y, c_z)], \quad c_x > 0 \tag{16}$$

Using a probabilistic interpretation, this boundary condition may be implemented as follows: deviational particles striking the boundary are specularly reflected with probability $(1-\alpha)$ or diffusely reflected with probability α. The fraction of deviational particles diffusely reflected (corresponding to n_b^d) can be treated using an algorithm similar to DSMC; i.e., particles striking the wall may be sent back to the computational domain drawn from the appropriate fluxal distribution (here, $c_x \phi^b, c_x > 0$). One important difference, however, is that only the *net* number of deviational particles is sent back into the domain since pairs of positive and negative particles correspond to zero net mass flux and can be cancelled, i.e.,

$$n_b^d \int_{c_x>0} c_x \phi^b d^3\mathbf{c} = -\int_{c_x<0} c_x f^d d^3\mathbf{c} \tag{17}$$

Equation (16) reveals a third contribution to the deviational population, namely, $\alpha[n_b^e f^b - F]$. This contribution is associated with the molecular flux incident upon the wall due to the underlying equilibrium distribution; n_b^e is determined from

$$n_b^e \int_{c_x>0} c_x \phi^b d^3\mathbf{c} = -\int_{c_x<0} c_x F d^3\mathbf{c} \tag{18}$$

As shown in Refs. [16,18], this case can be treated by creating deviational particles from the distribution $c_x[n_b^e \phi^b - F]$, $c_x > 0$. The number of particles per unit wall surface area generated in a time step is

$$\mathcal{F} = \frac{\alpha \Delta t}{N_{\mathrm{eff}}} \int_{c_x>0} c_x |n_b^e \phi^b - F| d^3\mathbf{c} \tag{19}$$

Let $M_{\max}$ bound the intergrand in Eq. (19) from above, c_a be a (positive) value such that the integrand is negligible for $\|\mathbf{c}\|_1 > c_a$, and A be the surface area of the boundary. The requisite number of particles is generated by repeating $\mathcal{N}_b = 4A M_{\max} c_a^3 \alpha \Delta t / N_{\mathrm{eff}}$ times:

1. Generate uniformly distributed, random velocity vectors $\mathbf{c}$ such that $\|\mathbf{c}\|_1 < c_a$ and $c_x > 0$.
2. If $c_x |n_b^e \phi^b(\mathbf{c}) - F(\mathbf{c})| > \mathcal{R} M_{\max}$, create a particle with velocity $\mathbf{c}$ and sign $\mathrm{sgn}[n_b^e \phi^b(\mathbf{c}) - F(\mathbf{c})]$. Generated particles are advected for a random fraction of a time step.

4 Results and Discussion

We have performed extensive validations and performance evaluations of the proposed method using a variety of test cases. Here, we present some representative transient and steady-state results involving heat exchange between two infinite, parallel walls at different temperatures (T_0 and $T_1 = T_0 + \Delta T$ where $\Delta T = \varepsilon T_0$) and a distance L apart in the x direction. The Knudsen number is defined as $k = c_0 \tau_0 / L$, where τ_0 is the collision time at the reference (absolute equilibrium) condition.

We start by discussing the variance reduction achieved by the present method. Validation is discussed in the following section.

4.1 Relative Statistical Uncertainty. As stated above and as shown in Refs. [11,16,18], deviational methods such as the one presented here exhibit statistical uncertainties that scale with the local deviation from equilibrium, thus allowing the simulation of arbitrarily low deviations from equilibrium at a cost that is independent of this deviation. Here, we demonstrate this feature by studying the statistical uncertainty of the temperature in a problem involving heat transfer.

Figure 1 shows the relative statistical uncertainty in the temperature ($\sigma_T / \Delta T = \sigma_T / (\varepsilon T_0)$) as a function of ε for steady-state heat exchange between the two walls ($k = 1, T_0 = 273$ K, $\alpha = 1$); σ_T is defined as the standard deviation in the temperature measured in two computational cells in the middle of the computational domain, each containing approximately $N = 950$ particles. Our results are compared with those from a representative nondeviational method, namely, DSMC. The DSMC performance is calculated from the theoretical result of Ref. [15] obtained using equilibrium statistical mechanics (assuming small deviation from equilibrium). We also performed DSMC simulations (of the relaxation-time model) to verify that this theoretical result remains accurate for $\varepsilon \gtrsim 0.1$. The figure shows that this is indeed the case, provided that in the equilibrium result [15],

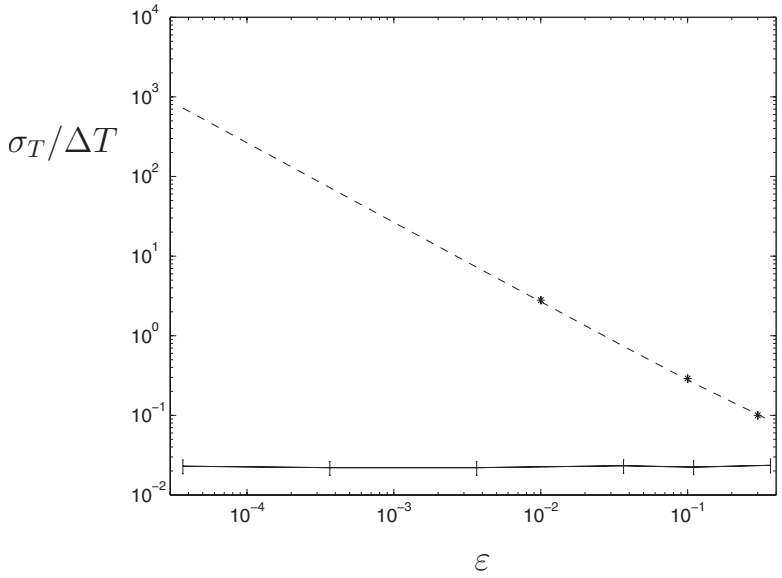

Fig. 1 The relative statistical uncertainty in temperature, $\sigma_T/\Delta T$, as a function of ε for steady-state heat exchange between two parallel plates at different temperatures with $k=1$, $\alpha=1$, and $T_0=273$ K. Simulation results (symbols with error bars on solid line) are presented and compared with the theoretical prediction [15] for DSMC (dashed line), which serves as a canonical case of a nondeviational method. Stars show actual DSMC results verifying that equilibrium theory is reliable up to at least $\varepsilon \approx 0.3$.

$$\sigma_T = \frac{T_0}{\sqrt{1.5N}} \tag{20}$$

T_0 is interpreted as the *local* temperature value.

Figure 1 also shows that for $\varepsilon \lesssim 0.3$ the relative statistical uncertainty of the deviational method proposed here remains essentially independent of ε, in sharp contrast to "nondeviational" methods. Moreover, the variance reduction achieved is such that significant computational savings are expected for $\varepsilon \lesssim 0.1$, particularly when considering that the cost savings scale with the square of the relative statistical uncertainty (since statistical noise decreases with the square root of the number of samples).

4.2 Validation. Figure 2 shows a comparison between the numerical solution of the linearized ($\varepsilon \ll 1$) relaxation-time model of the Boltzmann equation [27] and our simulation results for the heat flux between the two walls, q, for the case $\alpha=1$. The figure compares the heat flux normalized by the free-molecular (ballistic) value, $|q_{\mathrm{fm}}(\alpha)| = \alpha\varepsilon P_0 c_0/[\sqrt{\pi}(2-\alpha)]$, as a function of k; here, $P_0 = n_0 k_B T_0$ is the equilibrium gas pressure. The agreement between the two results is excellent.

Figure 3 shows a comparison for $\alpha=0.826$, one of the few cases for which numerical results for $\alpha \neq 1$ are readily available [28]. The agreement is again excellent.

Figure 4 shows a comparison between our simulation results and an analytical solution [29] of the linearized collisionless Boltzmann equation for oscillatory variation in the boundary tempera-

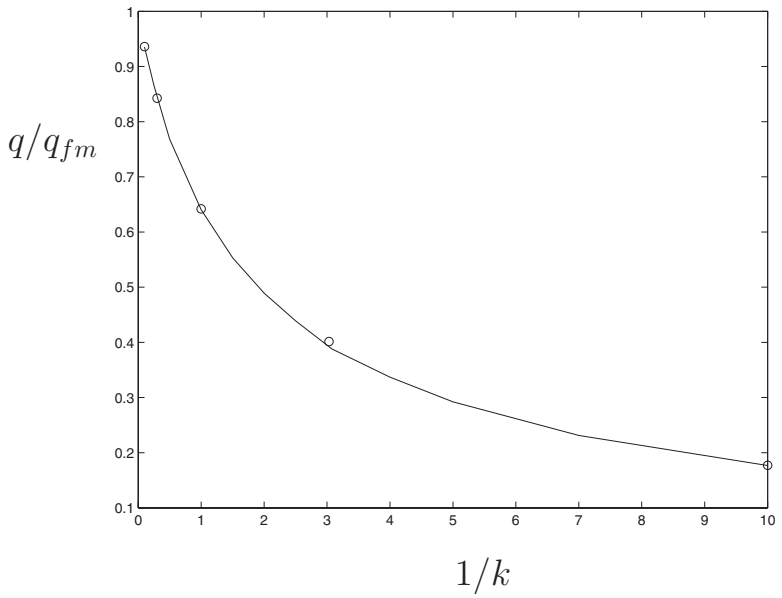

Fig. 2 Comparison between the numerical solution of the linearized Boltzmann equation by Bassanini et al. [27] (solid line) and simulation results (circles) for the heat flux between two parallel, infinite, fully accommodating walls. Some numerical solution data for $k>1$ have been transcribed from Ref. [20].

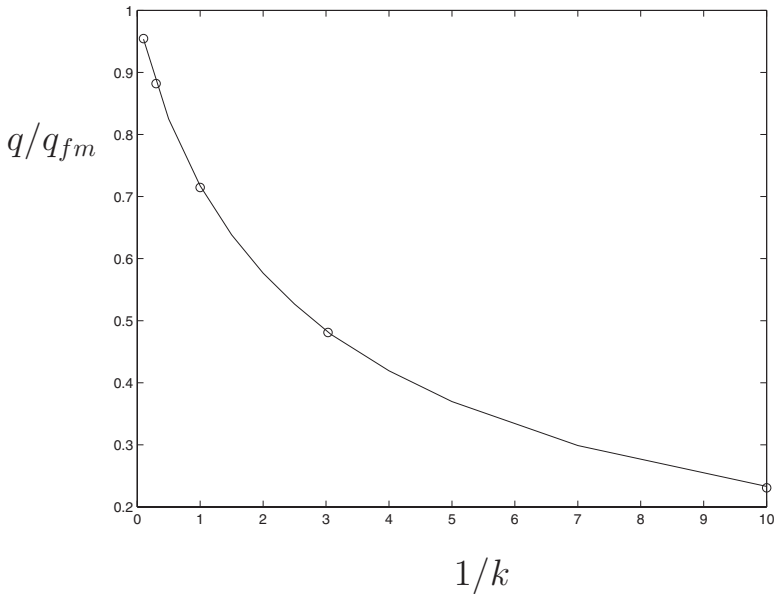

Fig. 3 Comparison between the numerical solution of the linearized Boltzmann equation by Bassanini et al. [28] (solid line) and simulation results (circles) for the heat flux between two parallel, infinite walls with $\alpha=0.826$

ture, i.e., $T_1=T_0(1+\varepsilon \sin \omega t)$, $\varepsilon \ll 1$, at a frequency ω that is large compared with the inverse acoustic (ballistic) system time scale ($\omega L/c_0 \gg 1$). The theoretical solution shows [29] that for sufficiently large frequencies, the hydrodynamic fields decay away from the wall proportionally to $\exp[-(\omega\delta_w/c_0)^{2/3}]$, where δ_w is the distance from the wall; in other words, "ballistic bounded layers" are formed (in contrast to Stokes layers, which are a result of diffusive transport). As a result, provided ω is sufficiently large, the collisionless description remains valid for systems of arbitrarily large size. Figure 4 shows a comparison between the theoretical results [29] and the simulation for $k=1$, $\alpha=1$, and $\omega L/c_0=40\pi$ for the density, flow velocity normal to the wall, temperature, and heat flux. The analytical solution is based on an asymptotic expansion valid for $\omega\delta_w/c_0 \gg 1$ [29]; thus, it is not valid in small regions close to the wall where the above condition is not satisfied. Our results show that sufficiently far from the wall, the agreement between theory and simulation is excellent.

As shown above, although the computational advantage of the method presented here compared with nondeviational methods increases as the deviation from equilibrium decreases, the amount of variance reduction achieved is such that considerable computational savings are obtained even when the deviation from equilibrium is not small. Below, we present a comparison between our results and DSMC simulations of the relaxation-time model in this latter regime. Specifically, we simulate an impulsive heating problem where at time $t=0$ the temperature of the wall at $x=-L/2$ jumps from T_0 to $T_0+\Delta T$; the gas is initially in equilibrium at temperature T_0, and both walls are fully accommodating ($\alpha=1$).

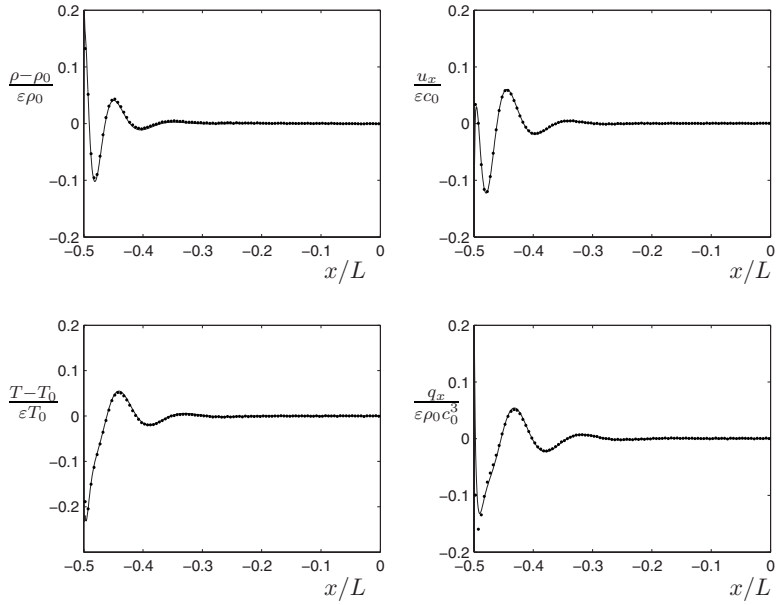

Fig. 4 Comparison between the proposed method (dots) and the theoretical results of Ref. [29] (solid lines) for $\omega L/c_0=40\pi$, $k=1$, $\alpha=1$, and $\varepsilon=0.02$. Here, $\rho_0=mn_0$.

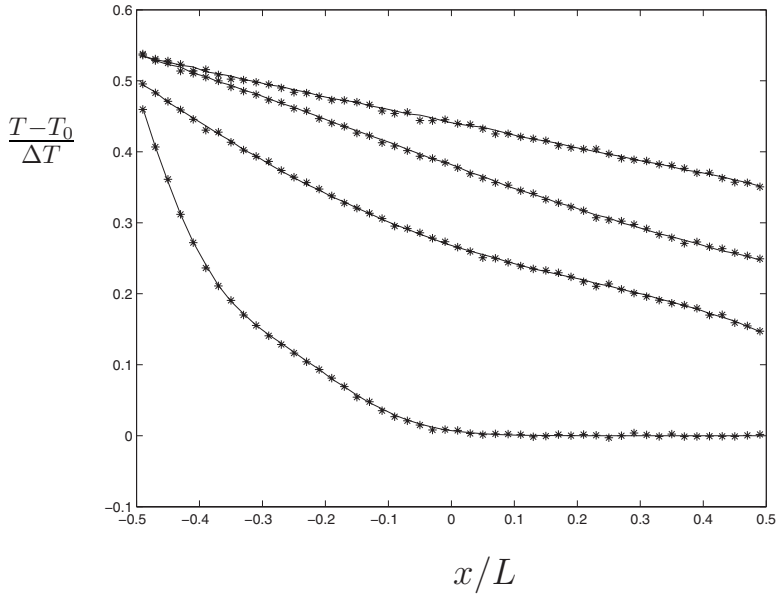

Fig. 5 Impulsive heating problem for $\varepsilon=0.1$ and $k=10$ at $t=0.02\tau_0$, $0.1\tau_0$, $0.2\tau_0$, and $0.4\tau_0$. The solid line denotes the present method, and stars denote DSMC results.

Figures 5–7 show a comparison between the two solutions for the transient evolution of the temperature field for $\varepsilon=0.1$ for $k=10$, $k=1$, and $k=0.1$, respectively. Figure 8 shows a comparison for $k=1$ and $\varepsilon=0.3$. This value of ε, which for $T_0=273$ K corresponds to $\Delta T=81.9$ K, places the deviation from equilibrium into the early nonlinear regime (previous work [5] shows that weakly nonlinear effects appear at $\varepsilon\approx 0.05$). The agreement between the two simulation approaches is excellent in all cases.

Although computational performance is always implementation dependent, an *indication* of the speedup achieved by the proposed method can be obtained by considering the following CPU times for calculations achieving a *relative* statistical uncertainty of 5% in the heat flux for $\varepsilon=0.01$: A transient variance-reduced calculation to time $t=2\tau_0$ at $k=0.1$ requires approximately 600 s on one core of a 3.0 GHz Intel Core 2 Quad processor; a calculation to $t=0.2\tau_0$ at $k=10$ requires approximately 40 s. In contrast, *with all discretization parameters the same* (and thus similar memory usage), DSMC requires approximately 150,000 s to reach the same final time ($t=2\tau_0$) at $k=0.1$ and 65,000 s for $k=10$($t=0.2\tau_0$). The CPU times for other values of ε can be estimated by noting that for small ε, these times are independent of ε for the proposed method, while for DSMC they scale approximately as ε^{-2}. In steady-state problems—where continuous sampling after steady state is reached can be performed—the speedup will in general be smaller because in the low-variance calculations the time to reach steady state becomes an appreciable part of the total simulation time.

4.3 A Comment on Linear Conditions. The algorithm described in this paper imposes no restrictions on the magnitude of

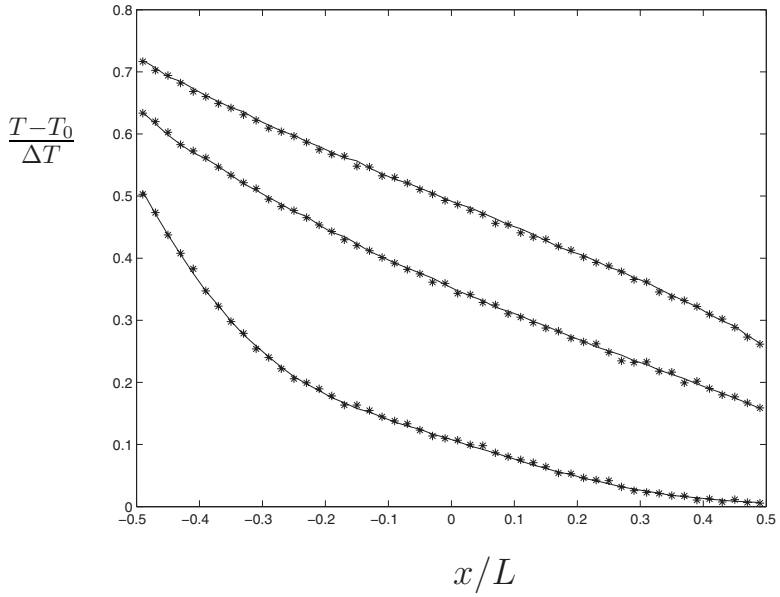

Fig. 6 Impulsive heating problem for $\varepsilon=0.1$ and $k=1$ at $t=0.4\tau_0$, $1.6\tau_0$, and $8\tau_0$. The solid line denotes the present method, and stars denote DSMC results.

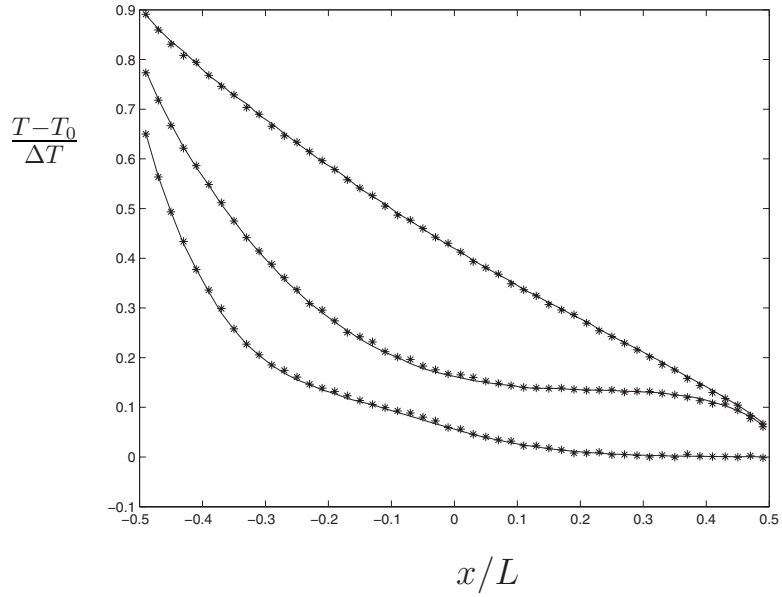

Fig. 7 Impulsive heating problem for $\varepsilon=0.1$ and $k=0.1$ at $t=4\tau_0$, $12\tau_0$, and $40\tau_0$. The solid line denotes the present method, and stars denote DSMC results.

f^d, although as discussed above, the deviational approach becomes significantly more efficient than traditional approaches when f^d is small. If f^d is sufficiently small for linearization to be appropriate, under some conditions, significant gains in computational efficiency can be achieved by considering the following. Under linear conditions, we can write

$$f^{\text{loc}} - F = F\left[\psi + 2\frac{\hat{\mathbf{c}}\cdot\mathbf{u}_{\text{loc}}}{c_0} + \left(\hat{\mathbf{c}}^2 - \frac{3}{2}\right)\theta\right] \tag{21}$$

where $\psi=n_{\text{loc}}/n_0-1$, $\hat{\mathbf{c}}=\mathbf{c}/c_0$, and $\theta=T_{\text{loc}}/T_0-1$. This representation can be very useful for improving the computational efficiency of update (Eq. (9)). For example, for isothermal constant density flows, particles may be generated from a combination of a normal distribution and analytic inversion of the cumulative distribution function, which is significantly more efficient than acceptance-rejection. Alternatively, Eq. (21) provides a means of obtaining bounds for $|f^{\text{loc}}-F|$, i.e., $\Delta_{\max}$, and thus reducing the number of rejections if the acceptance-rejection route is followed.

5 Conclusions

We have presented an efficient variance-reduced particle method for solving the Boltzmann equation in the relaxation-time approximation. The method combines simplicity with a number of desirable properties associated with particle methods, such as robust capture of traveling discontinuities in the distribution function and efficient collision operator evaluation using importance sampling [11], without the high relative statistical uncertainty associated with traditional particle methods in low-signal problems.

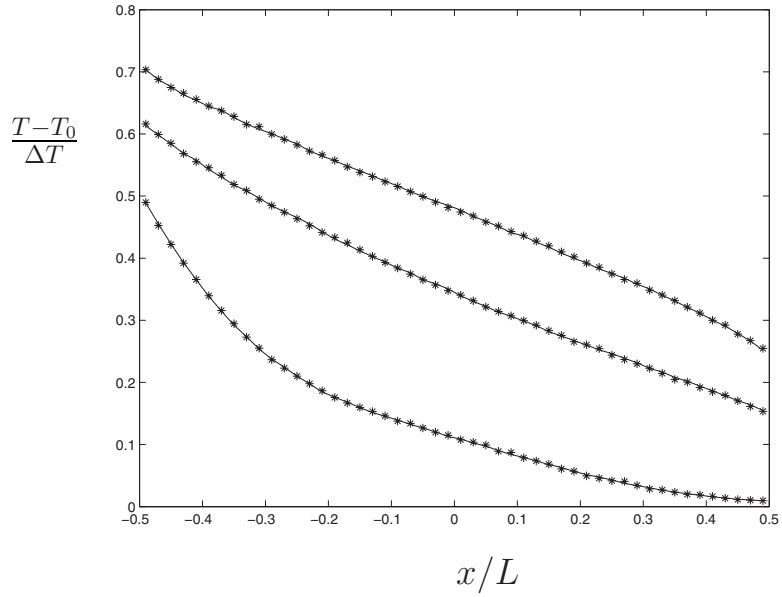

Fig. 8 Impulsive heating problem for $\varepsilon=0.3$ and $k=1$ at $t=0.4\tau_0$, $1.6\tau_0$, and $8\tau_0$. The solid line denotes the present method and stars denote DSMC results.

In particular, as shown above, the method presented here can capture arbitrarily small deviations from equilibrium at a cost that is independent of the deviation from equilibrium.

Future work will concentrate on further improving the efficiency of deviational methods. Recent work [30] shows that the ratio-of-uniforms method [31] can yield significant efficiency improvements in sampling distributions, while simulating the deviation from a spatially variable equilibrium distribution reduces the number of particles required to achieve the same statistical uncertainty.

Acknowledgment

This work was supported by the Singapore-MIT Alliance under the HPCES program.

Nomenclature

A = surface area of the boundary
$\boldsymbol{a}$ = acceleration due to an external field
$\boldsymbol{c}$ = molecular velocity vector
f = single-particle distribution function
F = absolute equilibrium distribution
k = Knudsen number ($=c_0\tau_0/L$)
k_B = Boltzmann's constant
L = plate separation
m = molecular mass
$M_{\max}$ = upper bound on the difference between fluxal distributions
n = number density
N = number of particles
N_{eff} = effective number of physical deviational particles per computational particle
$\mathcal{N}$ = number of trial particles
P = pressure
$\boldsymbol{q}$ = heat flux
$\boldsymbol{r}$ = position vector in physical space
$\mathcal{R}$ = random number uniformly distributed on $[0,1]$
t = time
T = temperature
$\boldsymbol{u}$ = flow velocity vector
$\mathcal{V}_{\text{cell}}$ = cell volume

Greek

α = accommodation coefficient
δ_w = distance from the wall
$\Delta_{\max}$ = upper bound on the difference between distributions
ε = dimensionless temperature difference ($=\Delta T/T_0$)
θ = dimensionless temperature ($=T_{\text{loc}}/T_0-1$)
τ = relaxation time
σ = standard deviation
ϕ = probability distribution function
ω = oscillation frequency
ψ = dimensionless density ($=n_{\text{loc}}/n_0-1$)

Subscripts and Superscripts

b = boundary
c = collision
d = deviational
e = equilibrium
fm = free molecular
loc = local
0 = absolute equilibrium

References

[1] Chen, G., 2005, *Nanoscale Energy Transport and Conversion*, Oxford University Press, New York.
[2] Majumdar, A., 1993, "Microscale Heat Conduction in Dielectric Thin Films," ASME J. Heat Transfer, **115**, pp. 7–16.
[3] Chen, G., 2002, "Ballistic-Diffusive Equations for Transient Heat Conduction From Nano to Macroscales," ASME J. Heat Transfer, **124**, pp. 320–328.
[4] Haji-Sheikh, A., Minkowycz, W. J., and Sparrow, E. M., 2002, "Certain Anomalies in the Analysis of Hyperbolic Heat Conduction," ASME J. Heat Transfer, **124**, pp. 307–319.
[5] Manela, A., and Hadjiconstantinou, N. G., 2007, "On the Motion Induced in a Gas Confined in a Small-Scale Gap Due to Instantaneous Heating," J. Fluid Mech., **593**, pp. 453–462.
[6] Hadjiconstantinou, N. G., 2002, "Constant-Wall-Temperature Nusselt Number in Micro and Nano Channels," ASME J. Heat Transfer, **124**, pp. 356–364.
[7] Hadjiconstantinou, N. G., 2003, "Dissipation in Small Scale Gaseous Flows," ASME J. Heat Transfer, **125**, pp. 944–947.
[8] Hadjiconstantinou, N. G., 2006, "The Limits of Navier-Stokes Theory and Kinetic Extensions for Describing Small-Scale Gaseous Hydrodynamics," Phys. Fluids, **18**, p. 111301.
[9] Hadjiconstantinou, N. G., 2000, "Analysis of Discretization in the Direct Simulation Monte Carlo," Phys. Fluids, **12**, pp. 2634–2638.
[10] Frangi, A., Frezzotti, A., and Lorenzani, S., 2007, "On the Application of the BGK Kinetic Model to the Analysis of Gas-Structure Interactions in MEMS," Comput. Struct., **85**, pp. 810–817.
[11] Baker, L. L., and Hadjiconstantinou, N. G., 2005, "Variance Reduction for Monte Carlo Solutions of the Boltzmann Equation," Phys. Fluids, **17**, p. 051703.
[12] Bird, G. A., 1994, *Molecular Gas Dynamics and the Direct Simulation of Gas Flows*, Clarendon, Oxford.
[13] Peterson, R. B., 1994, "Direct Simulation of Phonon-Mediated Heat Transfer in a Debye Crystal," ASME J. Heat Transfer, **116**, pp. 815–822.
[14] Mazumder, S., and Majumdar, A., 2001, "Monte Carlo Study of Phonon Transport in Solid Thin Films Including Dispersion and Polarization," ASME J. Heat Transfer, **123**, pp. 749–759.
[15] Hadjiconstantinou, N. G., Garcia, A. L., Bazant, M. Z., and He, G., 2003, "Statistical Error in Particle Simulations of Hydrodynamic Phenomena," J. Comput. Phys., **187**, pp. 274–297.
[16] Baker, L. L., and Hadjiconstantinou, N. G., 2008, "Variance-Reduced Particle Methods for Solving the Boltzmann Equation," J. Comput. Theor. Nanosci., **5**, pp. 165–174.
[17] Homolle, T. M. M., and Hadjiconstantinou, N. G., 2007, "Low-Variance Deviational Simulation Monte Carlo," Phys. Fluids, **19**, p. 041701.
[18] Homolle, T. M. M., and Hadjiconstantinou, N. G., 2007, "A Low-Variance Deviational Simulation Monte Carlo for the Boltzmann Equation," J. Comput. Phys., **226**, pp. 2341–2358.
[19] Cercignani, C., 1990, *Mathematical Methods in Kinetic Theory*, Plenum, New York.
[20] Cercignani, C., 1988, *The Boltzmann Equation and Its Applications*, Springer-Verlag, New York.
[21] Gurevich, V. L., 1986, *Transport in Phonon Systems*, North-Holland, New York.
[22] Lundstrom, M., 2000, *Fundamentals of Carrier Transport*, 2nd ed., Cambridge University Press, Cambridge.
[23] Davidson, B., and Sykes, J. B., 1957, *Neutron Transport Theory*, Clarendon, Oxford.
[24] Modest, M. F., 2003, *Radiative Heat Transfer*, 2nd ed., Academic, New York.
[25] Baker, L. L., and Hadjiconstantinou, N. G., 2008, "Variance Reduced Monte Carlo Solutions of the Boltzmann Equation for Low-Speed Gas Flows: A Discontinuous Galerkin Formulation," Int. J. Numer. Methods Fluids, **58**, pp. 381–402.
[26] Sone, Y., 2002, *Kinetic Theory and Fluid Dynamics*, Birkhauser, Boston.
[27] Bassanini, P., Cercignani, C., and Pagani, C. D., 1967, "Comparison of Kinetic Theory Analyses of Linearized Heat Transfer Between Parallel Plates," Int. J. Heat Mass Transfer, **10**, pp. 447–460.
[28] Bassanini, P., Cercignani, C., and Pagani, C. D., 1968, "Influence of the Accommodation Coefficient on the Heat Transfer in a Rarefied Gas," Int. J. Heat Mass Transfer, **11**, pp. 1359–1369.
[29] Manela, A., and Hadjiconstantinou, N. G., 2008, "Gas Motion Induced by Unsteady Boundary Heating in a Small-Scale Slab," Phys. Fluids, **20**, p. 117104.
[30] Radtke, G. A., and Hadjiconstantinou, N. G., 2009, "Variance-Reduced Particle Simulation of the Boltzmann Transport Equation in the Relaxation-Time Approximation," Phys. Rev. E, **79**, p. 056711.
[31] Wakefield, J. C., Gelfand, A. E., and Smith, A. F. M., 1991, "Efficient Generation of Random Variables via the Ratio-of-Uniforms Method," Stat. Comput., **1**, pp. 129–133.